Segregation in $(Fe_xMn_{1-x})_{35}Y_{65}$ metallic glasses determined by anomalous small-angle X-ray scattering

1989 J. Phys.: Condens. Matter 1 10249

(http://iopscience.iop.org/0953-8984/1/51/003)

J. Phys.: Condens. Matter **1** (1989) 10249–10263. Printed in the UK

Segregation in $(Fe_xMn_{1-x})_{35}Y_{65}$ metallic glasses determined by anomalous small-angle x-ray scattering

M Maret†, J P Simon† and O Lyon‡

† Laboratoire de Thermodynamique et Physico-Chimie Métallurgiques, CNRS and INPG, Ecole Nationale Supérieure d'Electrochimie et d'Electrométallurgie de Grenoble, BP 75, 38402 Saint Martin d'Hères, France

‡ Laboratoire d'Utilisation du Rayonnement Electromagnétique, CNRS, Bâtiment 209D, 91405 Orsay Cédex, France

Received 24 July 1989

Abstract. Small-angle x-ray scattering measurements were performed at the synchrotron source of the Laboratoire d'Utilisation du Rayonnement Electromagnétique in order to study the segregation occurring in the melt-spun $(Fe_xMn_{1-x})_{35}Y_{65}$ metallic glasses. The size of clusters ($r \simeq 7$ Å), the absence of an interference halo and the perfect representation of the scattered intensity by the Ornstein–Zernike law show that the morphology of the segregation is described in terms of concentration fluctuations and thus cannot be understood as a phase separation into two amorphous phases. These fluctuations are reinforced by the structural relaxation occurring after annealing at 573 K. From measurements using the anomalous dispersion technique, the partial atomic volume ratio V_{TM}/V_Y(TM ≡ Fe or Mn) in these glasses is found to be equal to 0.37, a value very close to the atomic size ratio in the pure metals and also to the ratio estimated from the inter-atomic distances determined by large-angle neutron scattering.

1. Introduction

The most direct technique using transmission electron microscopy (TEM) to study medium-range order in metallic glasses is small-angle x-ray scattering (SAXS) or small-angle neutron scattering (SANS) which are sensitive to fluctuations in scattering length density $\eta(r)$ (for a recent review of applications to metallic glasses, see Lamparter and Steeb (1988)). In a binary alloy the fluctuations of $\eta(r)$, the product of the local atomic scattering length $f(r)$ and the local atomic number density $\rho(r)$, are related to concentration fluctuations since $f(r)$ is equal to $C(r)f_1 + [1 - C(r)]f_2$ with $C(r)$ the local concentration and f_1 and f_2 the scattering lengths of the two species. In homogeneous binary glasses, the fluctuations of $C(r)$ and $\rho(r)$ can in fact be separated using the Bhatia–Thornton partial structure factors $S_{NN}(q)$, $S_{CC}(q)$ and $S_{NC}(q)$ (Bhatia and Thornton 1970), and the x-ray scattering intensity per atom can be expressed as

$$I(q) = \langle f\rangle\langle f^*\rangle S_{NN}(q) + \Delta f\,\Delta f^*\, C_1C_2S_{CC}(q) + 2\,\mathrm{Re}(\langle f\rangle\,\Delta f^*)S_{NC}(q) \qquad (1)$$

with $\langle f\rangle = C_1f_1 + C_2f_2$, $\Delta f = f_1 - f_2$ and where f^* and Δf^* are their complex conjugates.

In equation (1), the atomic number density fluctuations are described by $S_{NN}(q)$ and the concentration fluctuations by $S_{CC}(q)$. The Bhatia–Thornton functions have been

largely used to characterise the local order in liquid or amorphous alloys, and their long-wavelength limits ($q = 0$) are related to the thermodynamic properties of the alloy. Thus the limit at $q = 0$ of the x-ray scattering intensity per atom is given by

$$I(0) = \langle f \rangle \langle f^* \rangle \rho k_B T K_T + \mathrm{Re}[(\langle f \rangle \delta - \Delta f)(\langle f \rangle^* \delta - \Delta f^*)] C_1 C_2 S_{CC}(0) \tag{2}$$

with

$$S_{CC}(0) = \mathcal{N} k_B T / C_1 C_2 (\partial^2 G / \partial C_1^2)_{T,P}$$

ρ is the mean atomic number density, K_T the isothermal compressibility, G the Gibbs free energy per mole, k_B the Boltzmann constant, $\mathcal{N}$ the Avogadro number and δ defined by $\delta = (V_1 - V_2)/V_M$, with V_M the molar volume of the mixture and V_i the partial molar volumes.

For a random atomic distribution, $S_{CC}(0)$ is equal to unity; for tendency to hetero-coordination, $S_{CC}(0)$ takes values between zero and unity and, for tendency to segregation, $S_{CC}(0)$ is larger than unity. For a binary alloy above a miscibility gap, $S_{CC}(0)$ diverges when approaching the critical point and, at small q, $S_{CC}(q)$ follows the classical Ornstein–Zernike law (Stanley 1971):

$$S_{CC}(q) = S_{CC}(0)/(1 + \xi^2 q^2) \tag{3}$$

where ξ is the correlation length of concentration fluctuations. Therefore the large concentration fluctuations above a miscibility gap give rise to an increase in forward scattering.

In opposition with this thermodynamic approach, there is the case of a phase separation under a miscibility gap. In these two-phase systems, one generally approximates the pattern by N_p particles of volume ϑ_p with a homogeneous scattering length density η_p in a matrix of homogeneous scattering density η_m, and $I(q)$ is then given by

$$I(q) = (N_p \vartheta_p^2 / N)(\eta_p - \eta_m)(\eta_p - \eta_m)^* S(q) \tag{4}$$

where $S(q)$ is the Fourier transform of the pair correlation function of points situated in the particles (Patterson function) and N the total number of atoms in the alloy. Guinier and Fournet (1955) have shown that at small values of qR_G (R_G is the radius of gyration of the particle), $S(q)$ can be expressed as $S(q) = \exp(-q^2 R_G^2/3)$. Moreover, for particles with sharp boundaries, Porod has shown that $S(q)$ decreases at large q as q^{-4}.

In the present work, SAXS measurements are performed in as-quenched and annealed $(Fe_xMn_{1-x})_{35}Y_{65}$ metallic glasses. The structure of the Y-based glasses, characterised by a large ratio of the atomic volume of the transition metal (TM ≡ Mn, Fe, Ni and Cu) to the atomic volume of Y, was previously studied by large-angle neutron scattering (Maret *et al* 1987a, b). A continuous change in the local order was found so that $Ni_{33}Y_{67}$ is a chemically ordered glass, $Cu_{33}Y_{67}$ an almost randomly disordered glass and $(Fe_xMn_{1-x})_{35}Y_{65}$ segregating glasses. In these last alloys where the isomorphous behaviour between Fe and Mn atoms was checked, an increase in the total structure factor below around 0.5 Å^{-1} was observed whose importance depended on the ratio of Fe and Mn concentrations. The aim of these SAXS experiments is therefore to confirm and determine the origin of this signal at small q-vectors. The analysis of the SAXS results will be based on the two-phase approach and the Ornstein–Zernike theory. A few SAXS results in the $Ni_{33}Y_{67}$ and $Cu_{33}Y_{67}$ will be also presented in comparison with $(Fe_xMn_{1-x})_{35}Y_{65}$ and previous SANS results (Maret *et al* 1988).

Also, the technique of anomalous small-angle x-ray scattering (ASAXS), by tuning the x-ray energy at several values below the Fe or Mn absorption K edge, is used to vary

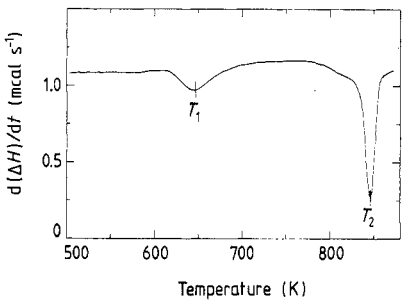

Figure 1. DSC thermogram of the $(Fe_{64}Mn_{36})_{35}Y_{65}$ metallic glass with a heating rate of 80 K min^{-1}. The first transformation corresponds to Y formation, and the second to the crystallisation of a Laves phase.

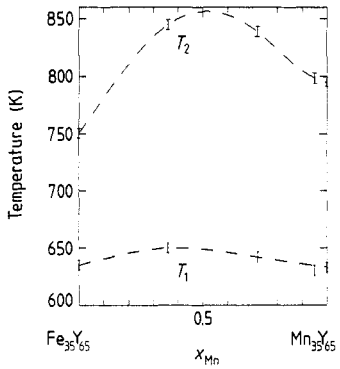

Figure 2. Evolution of the crystallisation temperatures of both reactions (see figure 1) against the Fe–Mn substitution (heating rate, 80 K min^{-1}).

the scattering contrast between late-transition-metal and Y atoms. The main advantage of the anomalous technique over the isotopic or isomorphic substitution in neutron diffraction is to make use of a unique sample (Simon *et al* 1985). For instance, one of the first applications of this ASAXS technique to metallic glasses was in hydrogenated CuTi glasses which allowed determination of the existence of titanium hydride small clusters (Goudeau *et al* 1987). Here, the anomalous measurements will allow us to estimate the ratio of the partial atomic volumes.

2. Experimental technique

2.1. Samples

Amorphous ribbons (1 mm wide and 20–30 μm thick) of $(Fe_xMn_{1-x})_{35}Y_{65}$ alloys (x = 1, 0.64 or 0.28) were cast on a rotating copper wheel of 286 mm diameter with a surface velocity of about 50 m s^{-1} under a He atmosphere. The crystallisation of the ternary glasses has been studied by differential scanning calorimetry (DSC). As shown for the $Fe_{64}Mn_{36})_{35}Y_{65}$ alloy in figure 1, it occurs in two steps as for the binary glass $Fe_{36}Y_{65}$ previously studied by Tenhover (1981) where the first transformation is associated with the formation of the HCP Y phase and an Fe-enriched amorphous phase and the second transformation to the formation of the Laves phase YFe_2. Since the equilibrium phases surrounding the eutectic composition close to 65 at.% Y are similar in the Fe–Y and Mn–Y systems (namely the HCP Y phase and the Laves phase) the same crystallisation reactions are expected in the ternary glasses. In figure 2, we report the crystallisation temperatures T_1 and T_2 of both reactions as a function of Mn concentration, obtained with a scan rate of 80 K min^{-1}. While T_1 changes very little with Mn concentration, an enhancement of the stability of the (Fe–Mn)-enriched amorphous phase remaining after the primary crystallisation of Y is observed in the ternary glasses.

Ribbons of $(Fe_xMn_{1-x})_{35}Y_{65}$ were heat treated at two temperatures lower than the crystallisation temperature (473 and 513 K) for 1 h. Typical DSC curves obtained in the

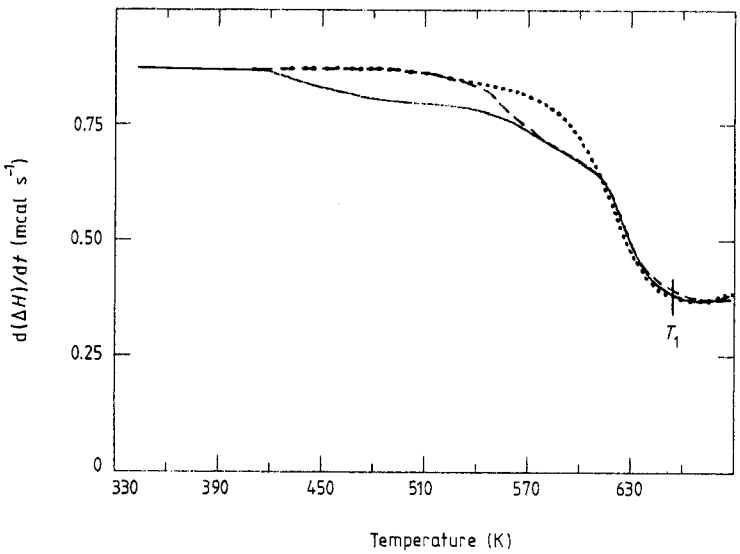

Figure 3. Exothermic effects measured by DSC with a heating rate of 80 K min^{-1} in as-quenched (——) and annealed ribbons (– – –, 473 K for 1 h; · · · ·, 513 K for 1 h) of $(Fe_{64}Mn_{36})_{35}Y_{65}$.

annealed $(Fe_{64}Mn_{36})_{35}Y_{65}$ ribbons are shown in figure 3. After the first heat treatment at 473 K, about 75% of the exothermic effect (associated with relaxation effects) is eliminated and after the heat treatment at 513 K the structural relaxation is almost complete. The same changes are roughly observed in the other glasses.

2.2. ASAXS measurements

The ASAXS experiments were performed on beam line D22 of the synchrotron radiation facility of Laboratoire d'Utilisation du Rayonnement Electromagnétique, Orsay, using a double Ge_{111} monochromator and a linear position-sensitive detector coupled to a multi-channel analyser. The ASAXS measurements were carried out at energies from 6875 to 7104 eV below the Fe absorption edge (7112 eV) for $Fe_{35}Y_{65}$ and from 6261 to 6531 eV below the Mn absorption edge (6539 eV) for the ternary glasses. Use of two sample–detector distances of 122 and 215 mm has allowed us to measure the scattering intensity over a q-range from 4×10^{-2} to 1 Å^{-1}.

The as-prepared ribbon has a fairly ideal thickness for x-ray measurements in transmission; so a single piece of ribbon was centred in the x-ray beam. This important and delicate step was achieved by choosing a beam geometry of 0.5 mm high and 3 mm wide and by measuring the sample transmission as a function of its position (by two monitor scintillators facing polymer films, placed before and after the sample). These transmission measurements allow calibration of the monochromator by running through the Fe edge. Finally, for small-angle scattering measurements, the rear monitor was replaced by the linear detector without moving the sample.

The scattering intensities were corrected for background, for sample absorption and for detector efficiency $\varepsilon(q)$ in position and detector efficiency $\varepsilon(E)$ in photon energy (Lyon and Simon 1987). The $\varepsilon(q)$ function was deduced from the measurement of the

Table 1. Atomic scattering factors in the $Fe_{35}Y_{65}$ glass.

Energy (eV)	F_{Fe}	F_Y	$\cos\varphi$
6875	22.89	38.91	0.9989
6990	22.22	38.88	0.9990
7056	21.41	38.87	0.9991
7090	20.90	38.86	0.9991
7104	19.51	38.86	0.9992

Table 2. Atomic scattering factors in the $(Fe_{64}Mn_{36})_{35}Y_{65}$ and $(Fe_{28}Mn_{72})_{35}Y_{65}$ glasses.

Energy (eV)	$(Fe_{64}Mn_{36})_{35}Y_{65}$			$(Fe_{28}Mn_{72})_{35}Y_{65}$		
	F_{TM}	F_Y	$\cos\varphi$	F_{TM}	F_Y	$\cos\varphi$
6261	23.36	39.04	0.9984	22.66	39.04	0.9984
6423	22.93	39.00	0.9986	21.98	39.00	0.9985
6492	22.57	38.99	0.9986	21.,36	38.99	0.9986
6520	22.25	38.98	0.9987	20.75	38.98	0.9987
6531	22.02	38.98	0.9987	20.30	38.98	0.9987

fluorescence of a Fe foil at 7500 eV and $\varepsilon(E)$ from the scattering measurement of a non-anomalous scatterer (Al–Ag foils which exhibit an interference peak in the investigated q-range). In order to determine the scattering intensity in absolute units (electrons squared per atom per steradian), the data are normalised from the Fe fluorescence (Simon and Lyon 1989). The q-independent contributions of the sample fluorescence and resonant Raman scattering were subtracted by assuming an asymptotic behaviour of the sample scattering in q^{-4} beyond 0.5 $Å^{-1}$.

2.3. Atomic scattering factors

At small scattering vectors, the x-ray atomic scattering factor is independent of q and is given by

$$f_i(E) = Z_i + f_i'(E) + if_i''(E).$$

E is the energy of photon beam, Z_i is the atomic number, and $f_i'(E)$ and $f_i''(E)$ are the dispersion terms of species i. For energies lower than the absorption edge, $f_i''(E)$ related to the absorption remains nearly constant, while $f_i'(E)$ can become as large as $7e$ near a K edge. The scattering factor of the isomorphous transition-metal mixture is given by

$$f_{TM}(E) = xf_{Fe}(E) + (1 - x)f_{Mn}(E).$$

$f_i(E)$ can be rewritten as $f_i(E) = F_i(E)\exp(i\varphi_i)$ and the coefficients in equations (1), (2) and (4) are simply expressed as function of $F_{TM}(E)$, $F_Y(E)$ and $\cos[\varphi(E)]$ where $\varphi(E) = \varphi_{TM}(E) - \varphi_Y(E)$. The values $F_{TM}(E)$ for the Fe atoms or for the mixture of Fe–Mn, $F_Y(E)$ and $\cos[\varphi(E)]$, corresponding to the different photon energies are calculated from the tables of Sazaki (1984) and reported in tables 1 and 2. The values have been

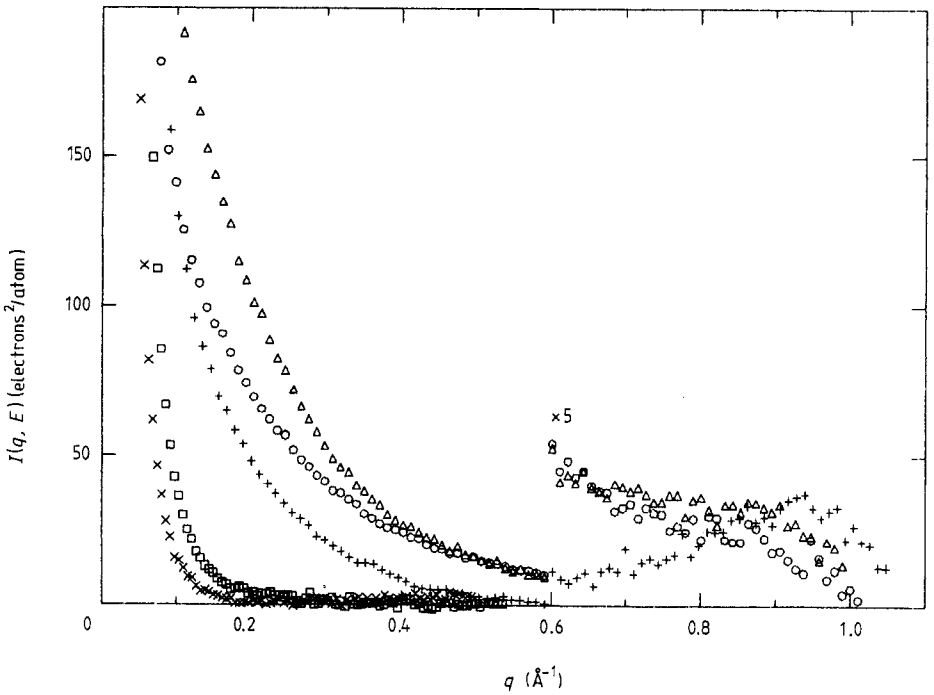

Figure 4. Intensity against momentum transfer for as-quenched metallic glasses: +, $Fe_{35}Y_{65}$; △, $(Fe_{64}Mn_{36})_{35}Y_{65}$; ○, $(Fe_{28}Mn_{72})_{35}Y_{65}$; □, $Cu_{33}Y_{67}$; ×, $Ni_{33}Y_{67}$.

corrected to take into account the wide band width of the Ge_{111} monochromator as done by Simon and Lyon (1989). Let us note that the imaginary term $f_i''(E)$ is negligible with regard to $Z_i + f_i'(E)$ for both species ($\cos\varphi \simeq 1$); so, to shorten the following, we shall use F_i instead of f_i.

3. Experimental results

Figure 4 shows the average curves obtained on an edge for the melt-spun $(Fe_xMn_{1-x})_{35}Y_{65}$ ($x = 0.28$, 0.64 and 1), $Cu_{33}Y_{67}$ and $Ni_{33}Y_{67}$ alloys. The intensities rapidly decrease with increasing momentum transfer q at small q and then more smoothly and slowly at larger q. The $I(q)$ behaviour is more explicit in a log–log plot (figure 5) and for the $(FeMn)_{35}Y_{65}$ glasses we observe changes in the scattering law which allow us to define the three following q-ranges: $q_1 < 0.1$ Å^{-1}, 0.1 Å$^{-1} \leqslant q_2 \leqslant 0.6$ Å^{-1} and $q_3 > 0.6$ Å^{-1}, discussed separately.

3.1. Low-q range $q < 0.1$ Å^{-1}

The interpretation of the signal at very small q-vectors about in q^{-n} (figure 5) is always problematic because of the contribution of surface states ($n = 4$) which adds to the bulk contribution. For the $Cu_{33}Y_{67}$ and $Ni_{33}Y_{67}$ glasses, the law in q^{-n} (with $n = 3.3$) is checked over a large q-range (in agreement with previous neutron scattering measurements

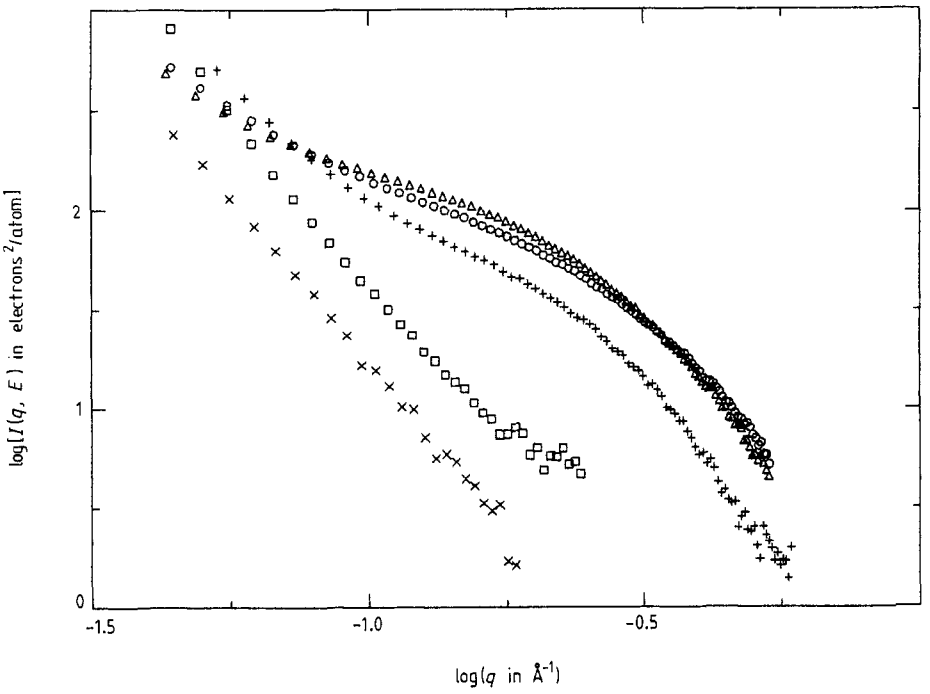

Figure 5. Log–log plot of the data in figure 4. The symbols have the same meanings as in figure 4.

(Maret *et al* 1988)). It can be interpreted as the sum of two contributions: a surface scattering in q^{-4} attributed mainly to yttrium oxide particles, and a bulk scattering in q^{-3}. The law in q^{-3} was observed for the first time in $TbCu_{3.54}$ glass (Boucher *et al* 1983) and interpreted as the existence of a profile of scattering length density within large domains. As previously found, in comparison with $Ni_{33}Y_{67}$, $Cu_{33}Y_{67}$ exhibits a reinforced signal which has been attributed to particles of a metastable phase of stoichiometry close to Y_3Cu_2 in the amorphous matrix (of about 150 Å diameter) using the Guinier approximation. In the case of $(Fe_xMn_{1-x})_{35}Y_{65}$, Y_2O_3 particles also contribute to the increase in $I(q)$ at very small q, since Bragg reflections of the hexagonal Y_2O_3 phase have been detected, superimposed on the neutron total structure factor of the amorphous alloy. However, the law in q^{-n} does not hold beyond about 0.1 $Å^{-1}$ (figure 5). Indeed, while the scattering of $Ni_{33}Y_{67}$ and $Cu_{33}Y_{67}$ becomes negligible beyond 0.15 $Å^{-1}$, the scattering of $(FeMn)_{35}Y_{65}$ is still important up to 0.6 $Å^{-1}$ and, as shown by the log–log representation, does not vary as q^{-n}; therefore the pair interactions, preferentially heteroatomic in $Ni_{33}Y_{67}$ and $Cu_{33}Y_{67}$, give rise to a local order which does not contribute to small-angle scattering. By contrast, the tendency towards segregation in $(FeMn)_{35}Y_{65}$ produces a small-angle scattering signal dominant between 0.15 and 0.6 $Å^{-1}$ which will be discussed in § 3.3.

3.2. High-q range $q > 0.6$ Å^{-1}

Let us examine the other limit, the large-q range. Beyond 0.6 $Å^{-1}$, only the $Fe_{35}Y_{65}$ glass exhibits an interference ring centred at about 0.9 $Å^{-1}$ which can be interpreted as the

existence of very small clusters with a separation distance of $2\pi/0.9 = 7$ Å. Such a ring has already been observed in the total structure factors of the $Fe_{35}Y_{65}$ and $(Fe_{64}Mn_{36})_{35}Y_{65}$ glasses measured by neutron diffraction (Maret *et al* 1987b) but disappeared in $(Fe_{28}Mn_{72})_{35}Y_{65}$. The intensity variation with isomorphous substitution was consistent with a small amount of YH_2 particles (between 0.4 and 0.7 mol% H_2). On the contrary, in the case of x-rays, the variation in contrast between YH_2 and the amorphous matrix with Mn content must be very weak; consequently such a halo should also be measurable in all glasses. It is believed that the very large background correction, added to the tail of the signal in the medium-q-range (which is higher in the ternary glasses), may give such a large noise-to-signal ratio that the interference ring was not detected in the ternary glasses. Supplementary measurements on an intermediate-q range covering the whole interference ring (i.e. $0.5\ \text{Å}^{-1} < q < 2\ \text{Å}^{-1}$) are therefore required to confirm its existence in these ternary glasses.

3.3. Intermediate-q-range 0.1 Å^{-1} ≤ q ≤ 0.6 Å^{-1}

In this q-range, the log–log plots show a continuous curvature for the three $(FeMn)_{35}Y_{65}$ glasses. So we tried different approaches to fit this signal with segregation. First we can assume the existence of a phase separation with yttrium-enriched regions in the amorphous matrix; it is supported by the fact that the crystallisation of these glasses starts with the crystallisation of the Y HCP phase. The two-phase approach has also been mostly used to interpret the small-angle scattering of amorphous alloys in the same q-range (see, e.g., Flank *et al* 1984, Goudeau *et al* 1987, Lamparter *et al* 1988b).

Guinier fits for the three as-quenched glasses (figure 6) are quite good and yield the particle radii R_g of gyration and the intensities $I(0)$ extrapolated at $q = 0$ listed in table 3 where the results of the annealed samples are also reported. R_g, which is small in the as-quenched samples (about 6–7 Å), decreases slightly after heat treatment, while $I(0)$, equal to $N_p\vartheta_p^2(\eta_p - \eta_m)^2/N$, increases to almost 50% (figure 7) owing to either a larger number of Y-enriched precipitates or an increase in the scattering contrast $\eta_p - \eta_m$. We shall point out significant differences in the scattering changes of the three $(Fe_xMn_{1-x})_{35}Y_{65}$ glasses. The heat treatment at the lowest temperature (473 K) has little influence on the ternary glasses (shown only for the $(Fe_{64}Mn_{36})_{35}Y_{65}$ glass in figure 7(*b*)) contrary to the case of the $Fe_{35}Y_{65}$ glass (figure 7(*a*)). These differences disappear at higher temperatures, since after the treatment at 513 K the SAXS intensity increases by the same order of magnitude in the three glasses with regard to as-quenched states.

A more accurate description of these Y-enriched regions necessitates determination of their composition and their volume fraction. From the Guinier law, we have an estimate of $I(0, E)$ which can be rewritten using equation (4) with $\cos\varphi = 1$ as

$$I(0,E) = (N_p\vartheta_p^2/N)(C_p^{TM}V_{TM}/V_p - C_m^{TM}V_{TM}/V_m)^2[F_{TM}(E)/V_{TM} - F_Y/V_Y]^2 \qquad (5)$$

if the partial atomic volumes V_{TM} and V_Y of both types of atom are equal in the Y-enriched particles and the amorphous matrix. The term $(C_p^{TM}V_{TM}/V_p - C_m^{TM}V_{TM}/V_m)^2$ depends on the atomic concentrations in the two phases (with $V_p = C_p^{TM}V_{TM} + C_p^{Y}V_Y$ and $V_m = C_m^{TM}V_{TM} + C_m^{Y}V_Y$) and the term in square brackets on the scattering lengths of both species.

If we assume spherical particles of pure yttrium ($C_p^{TM} = 0$), it is then possible to determine the volume fraction $f_p = N_p\vartheta_p/NV_a$, with V_a (= 24.8 Å^3) the mean atomic volume of the amorphous alloys, since C_m^{TM} is related to f_p by $C_m^{TM}V_{TM}/V_m = C_{TM}V_{TM}/[V_a(1 - f_p)]$ with C_{TM}, the nominal composition of transition-metal atoms. Using the

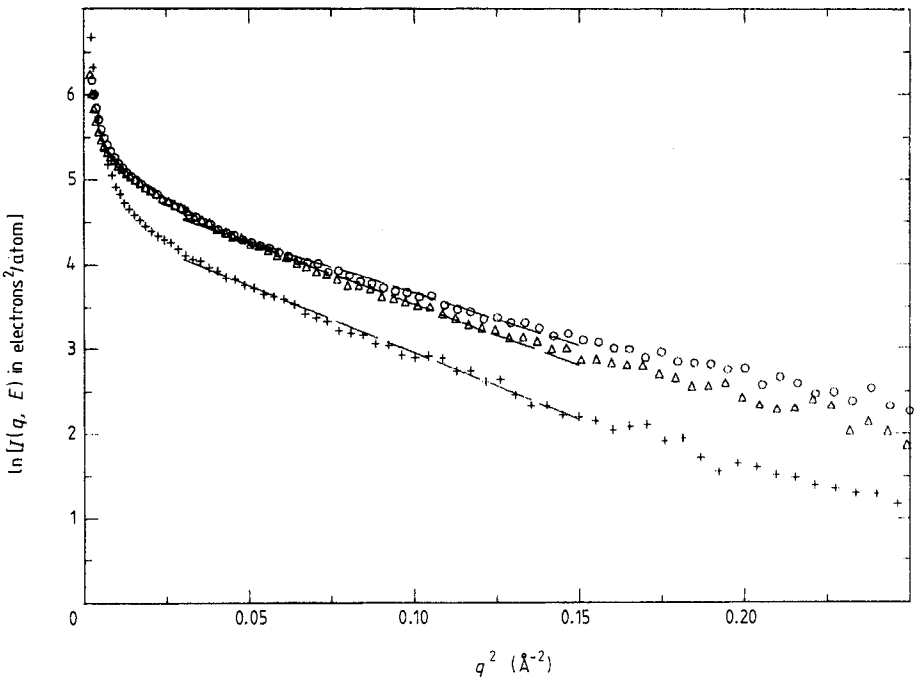

Figure 6. The Guinier analysis of the SAXS signal for three as-quenched glasses: +, $(Fe_{35}Y_{65})$; △, $(Fe_{64}Mn_{36})_{35}Y_{65}$; ○, $(Fe_{28}Mn_{72})_{35}Y_{65}$; – – –, best fit in the range $0.175\ Å^{-1} < q < 0.4\ Å^{-1}$.

values in tables 2 and 3, and the ratios V_{TM}/V_Y determined from anomalous dispersion (see § 4), the volume fractions are estimated at 0.1 and 0.13 in the as-quenched glasses for x equal to 0.64 and 0.28, respectively. If the particles still contain some TM atoms, their volume fraction should be found to be higher in order to balance the decrease in $\eta_p - \eta_m$. Consequently the volume fractions estimated above are the minimal values to produce the measured intensities. From the scaling function calculated by Rikvold and Gunton (1982) which describes systems undergoing phase separation, a volume fraction of 0.1 yields necessarily an interference halo relatively important in the inter-particle structure factor. The absence of such a halo demonstrates that the $(Fe_xMn_{1-x})_{35}Y_{65}$ glasses cannot be described as two-phase systems. In the following, we shall show that the SAXS intensities can be better interpreted in terms of compositional and density fluctuations.

The application of the Ornstein–Zernicke theory to the microscopic concentration fluctuations in disordered alloys yields the following expression for $I(q)$ in the small-q region (from equations (2) and (3)):

$$I(q) = A + B/(1 + \xi^2 q^2). \tag{6}$$

The first term of compressibility in equation (2) has been roughly included in the correction for fluorescence and Raman resonance. The plots of $[I(q) - A]^{-1}$ against q^2 shown in figure 8 correspond to the scattering intensities of the three as-quenched glasses averaged over the five energies below the Fe or Mn edge. For each glass, the linear behaviour observed in the almost whole q-range indicates that the Ornstein–Zernike equation is valid, and it holds also for the annealed samples, giving B and ξ with an accuracy of about 5%.

Table 3. Values of particle radius R_g of gyration and $I(0)$ deduced from the Guinier fits for the different states of the $(Fe_xMn_{1-x})_{35}Y_{65}$ alloys.

	$Fe_{35}Y_{65}$ (6875 eV)		$(Fe_{64}Mn_{36})_{35}Y_{65}$ (6261 eV)		$(Fe_{28}Mn_{72})_{35}Y_{65}$ (6261 eV)	
Alloy	R_g (Å)	$I(0)$ (electron^2/atom)	R_g (Å)	$I(0)$ (electron^2/atom)	R_g (Å)	$I(0)$ (electron^2/atom)
As-quenched	6.9	94.41	6.6	146	6.2	126
Annealed for 1 h at 473 K	6.9	116.1	6.5	160	6.2	138
Annealed for 1 h at 513 K	6.8	130	6.1	210	6.0	190

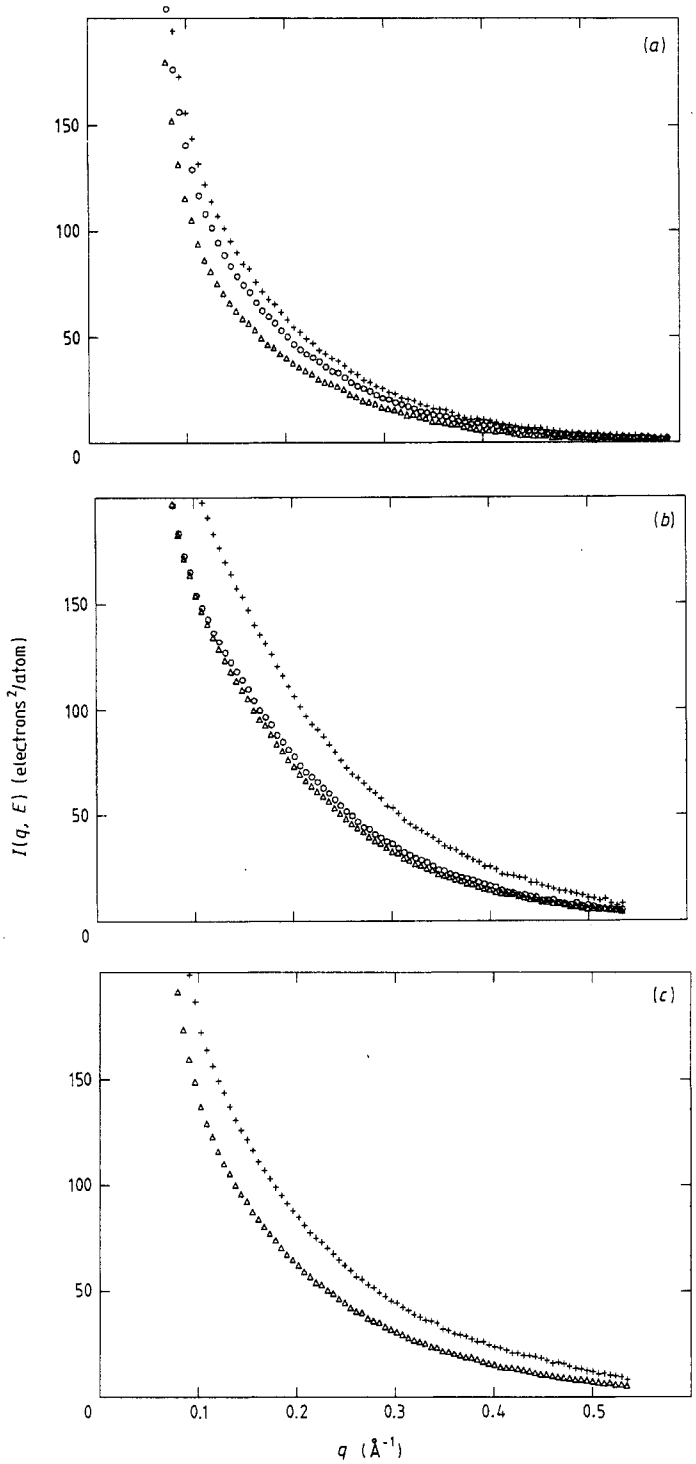

Figure 7. Effect of different heat treatments on the small-angle scattering of (*a*) $Fe_{35}Y_{65}$, (*b*) $(Fe_{64}Mn_{36})_{35}Y_{65}$ and (*c*) $(Fe_{28}Mn_{72})_{35}Y_{65}$: △, as-quenched; ○, annealed at 473 K for 1 h; +, annealed at 513 K for 1 h.

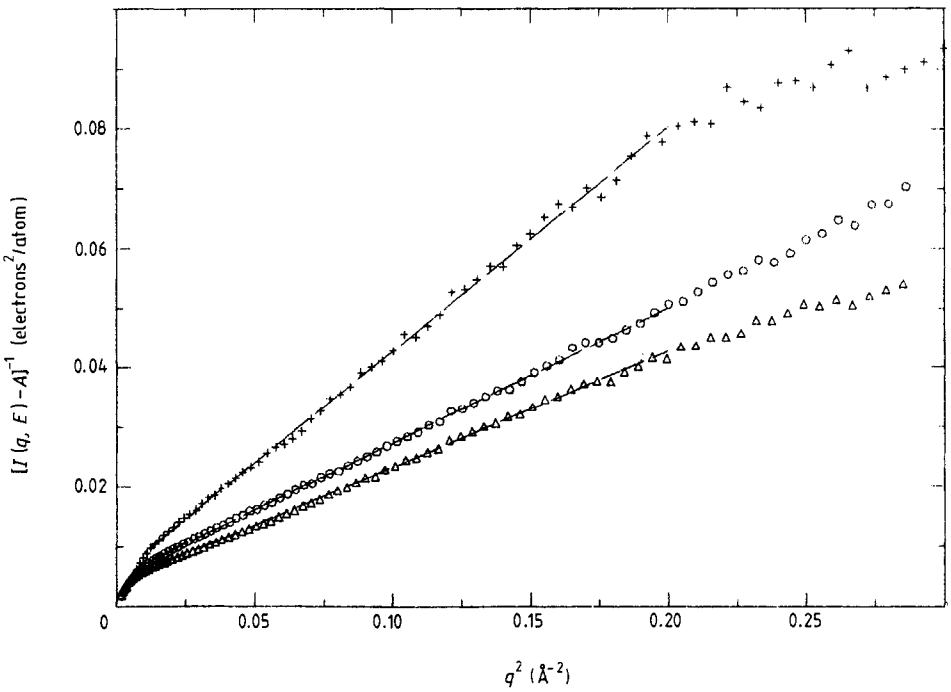

Figure 8. Ornstein–Zernike analysis for three as-quenched glasses: +, $Fe_{35}Y_{65}$; △, $(Fe_{64}Mn_{36})_{35}Y_{65}$; ○, $(Fe_{28}Mn_{72})_{35}Y_{65}$; – – –, best fit in the range 0.1 Å^{-1} < q < 0.45 Å^{-1}.

Table 4. Correlation lengths and limits at $q = 0$ of the concentration–concentration structure factor deduced from the Ornstein–Zernike plots in as-quenched and annealed samples.

	$F_{35}Y_{65}$		$(Fe_{64}Mn_{36})_{35}Y_{65}$		$(Fe_{28}Mn_{72})_{35}Y_{65}$	
Alloy	ξ (Å)	$S_{CC}(0)$	ξ (Å)	$S_{CC}(0)$	ξ (Å)	$S_{CC}(0)$
As-quenched	8.5	7.6	7.2	8.1	6.9	9
Annealed for 1 h at 473 K	8.9	10	6.8	8.1		
Annealed for 1 h at 513 K	8.5	10.8	6	9.5	5.7	9.9

The long-wavelength limit $S_{CC}(0)$ is deduced from the following expression for B using equation (2) and the definition of $\delta = (V_{TM} - V_Y)/(C_{TM}V_{TM} + C_YV_Y)$:

$$B = (F_{TM}/V_{TM} - F_Y/V_Y)^2[V_YV_{TM}/(C_{TM}V_{TM} + C_YV_Y)]^2C_{TM}C_YS_{CC}(0). \quad (7)$$

The values of the correlation length ξ and the long-wavelength limit $S_{CC}(0)$ are reported in table 4. The change in ξ for the three glasses between the different states is quite similar to the change in R_G in the Guinier approximation. Let us also emphasise that the scattering contrast is of the same form $(F_{TM}/V_{TM} - F_Y/V_Y)^2$, as in the two-phase model. The correlation length is always shorter in the ternary glasses than in the binary glass and, except for $Fe_{35}Y_{65}$, decreases after annealing treatments. The values of $S_{CC}(0)$ much larger than unity confirm the segregation between TM and Y atoms. Contrary to the simultaneous increase in ξ and $S_{CC}(0)$ observed in binary crystalline or liquid alloys

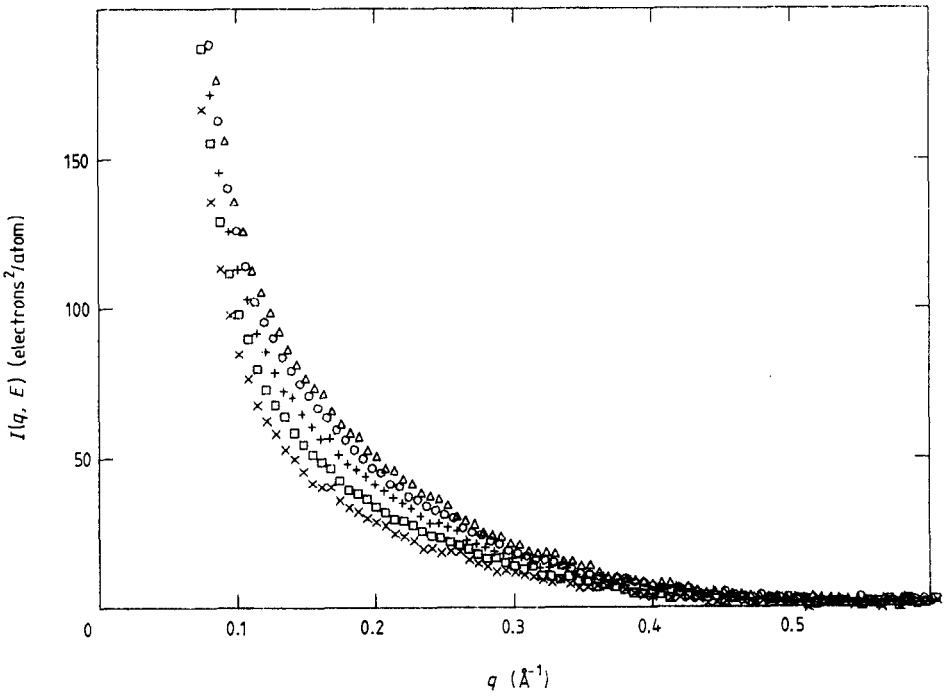

Figure 9. Change in the scattering intensity with photon energy near the Fe K absorption edge (7112 eV) in the as-quenched $Fe_{35}Y_{65}$ glass: △, 6875 eV; ○, 6990 eV; +, 7056 eV; □, 7090 eV; ×, 7104 eV.

when approaching a miscibility gap, we observe here an increase in concentration fluctuations together with a small decrease in ξ after annealing. Since the crystallisation of these glasses starts with the precipitation of the Y phase, we believe that the correlation length should increase after treatments at temperatures still closer to the crystallisation temperature. SAXS experiments are now planned in order to follow the variation in ξ and $S_{CC}(0)$ up to the onset of the primary crystallisation of the Y phase.

4. Results of the anomalous dispersion in the medium-q range

Figures 9 and 10 show the changes in the corrected scattering intensities with the photon energy for the as-quenched $Fe_{35}Y_{65}$ and $(Fe_{64}Mn_{36})_{35}Y_{65}$ glasses, respectively; there is an increase in $I(q, E)$ when moving away from the edge. As we have mentioned above, the SAXS intensity is proportional to the square of the fluctuations of scattering length density, whether these fluctuations are well formed particles (equation (5)) or these fluctuations are some kind of local order (equation (6)) and therefore proportional to $F_{TM}(E) - V_{TM}F_Y(E)/V_Y$, where V_{TM} and V_Y are the partial atomic volumes of the two species. From the atomic volumes in the pure components $V^0_{Fe} = 11.77$ Å^3, $V^0_{Mn} = 12.21$ Å^3 and $V^0_Y = 33.01$ Å^3), and from tables 1 and 2 we see that $V_{TM}F_Y(E)/V_Y$ is lower than $F_{TM}(E)$ and the difference $F_{TM}(E) - V_{TM}F_Y(E)/V_Y$ increases with $F_{TM}(E)$ when moving away from the edge.

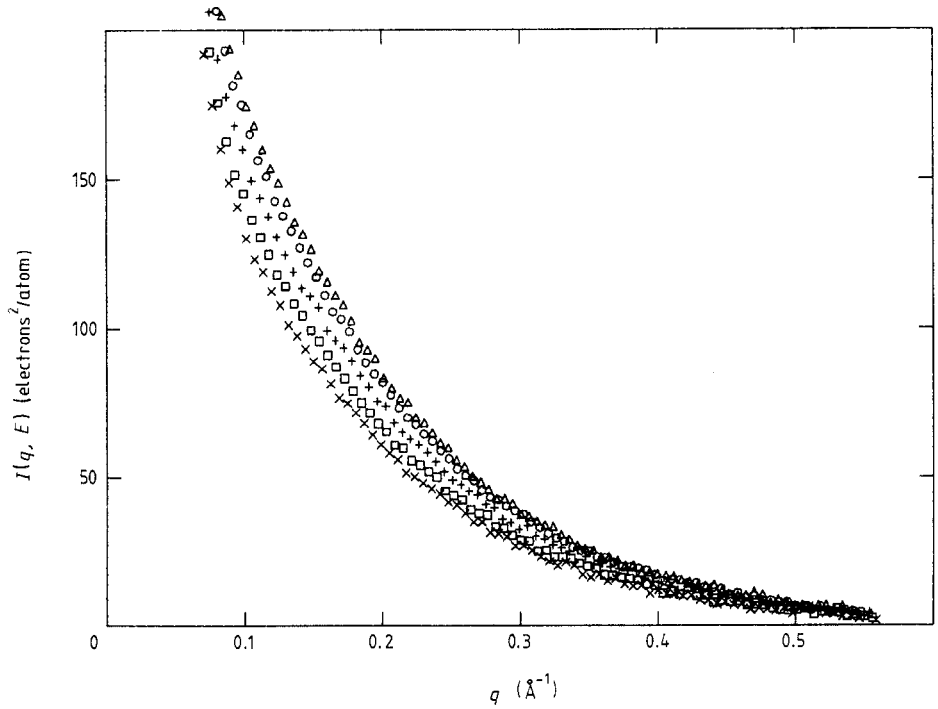

Figure 10. Change in the scattering intensity with photon energy near the Mn K absorption edge (6538 eV) in the as-quenched $(Fe_{64}Mn_{36})_{35}Y_{65}$ glass: △, 6261 eV; ○, 6423 eV; +, 6492 eV; □, 6520 eV; ×, 6531 eV.

The anomalous measurements near the transition-metal K edge allow us to determine the ratio of atomic volumes in the alloy from a linear correlation between $\sqrt{\Sigma_q I(q, E)}$ and $F_{TM}(E)$ (Lyon and Simon 1986). Using this method, V_{TM}/V_Y is found to be equal to 0.36 for $(Fe_{64}Mn_{36})_{35}Y_{65}$ and to 0.37 for $(Fe_{28}Mn_{72})_{35}Y_{65}$ and is therefore very close to the atomic volume ratios $V^0_{Fe}/V^0_Y = 0.356$ and $V^0_{Mn}/V^0_Y = 0.37$ of the pure components (the q-interval chosen for the calculation of $\Sigma_q I(q, E)$ is $0.06\ \text{Å}^{-1} \leqslant q \leqslant 0.5\ \text{Å}^{-1}$). However, for the binary glass, the ratio V_{Fe}/V_Y is strongly dependent on the choice of energies, since it is found to be equal to 0.3 or 0.17, respectively, by including or not including the measurement of $I(q)$ at 6492 eV in addition to the five measurements near the Fe edge. This variation in V_{Fe}/V_Y suggests that this series of ASAXS measurements in the $Fe_{35}Y_{65}$ glass does not allow us to extract a reliable value of V_{Fe}/V_Y, in part owing to the weaker scattering intensity level. Supplementary measurements at lower energies are then required in order to increase the scattering contrast between Fe and Y atoms.

Finally, the anomalous small-angle x-ray patterns of the annealed samples vary with energy as do those for the as-quenched samples. The ratio V_{TM}/V_Y does not significantly change after structural relaxation, in agreement with the very small atomic rearrangements observed by neutron diffraction (see, e.g., Lefèbvre *et al* 1988).

5. Conclusion

SAXS measurements have allowed us to determine the medium-range order in $(Fe_xMn_{1-x})_{35}Y_{65}$ glasses in terms of concentration and density fluctuations, yielding a

segregation between transition-metal and Y atoms extending over a distance of about 7 Å. By contrast, the absence of a SAXS signal above 0.15 $Å^{-1}$ for $Cu_{33}Y_{67}$ and $Ni_{33}Y_{67}$ is in agreement with previous neutron scattering results which showed a tendency to chemical order. For $(Fe_xMn_{1-x})_{35}Y_{65}$ glasses, the absence of an interference halo below 0.5 $Å^{-1}$ excludes phase separation into two amorphous phases, as was clearly observed in several amorphous alloys such as AuSi by TEM (Audier *et al* 1985) and $Au_{60}Pb_{20}Sb_{20}$ and $Pd_{60}Pd_{40}$ by SANS (Yavari 1988). In these alloys, the first peak of the total structure factor is split into two components; however, this was not observed for $(Fe_xMn_{1-x})_{35}Y_{65}$. It therefore indicates that the morphology of the segregation in $(Fe_xMn_{1-x})_{35}Y_{65}$ cannot be described by a narrow size distribution of precipitates as in unmixed systems but in terms of concentration fluctuations. This last interpretation might also hold in the case of as-quenched $Fe_{80}B_{20}$ glass (Lamparter *et al* 1988) where the weak SANS intensity without halo detected between 0.1 and 0.2 $Å^{-1}$ gives a radius of gyration of 4.8 Å in the Guinier approximation.

In annealed ribbons in which structural relaxation occurs, an increase in the concentration fluctuations is observed together with a slight decrease in their correlation length. The increase in concentration fluctuations indicates the development of the segregation. Nevertheless the decrease in the correlation length is unusual but might be correlated to a quenching effect; on crossing the glass transition, the system should be frozen in intermediate local clustering, i.e. with a ξ which is too large.

Finally from the anomalous measurements the partial atomic volume ratio V_{TM}/V_Y in the ternary glasses is found to be equal to 0.36 and to 0.37 for $x = 0.64$ and 0.28, respectively. These ratios, which are very close to the atomic volume ratio of the pure metals, are in fair agreement with the inter-atomic distances obtained from large-angle neutron scattering measurements (Maret *et al* 1987b).

References

Audier M, Guyot P, Simon J P and Valignat N 1985 *J. Physique Coll.* **46** C8 433
Bhatia A B and Thornton D E 1970 *Phys. Rev.* B **2** 3004
Boucher B, Chieux P, Convert P and Tournarie M 1983 *J. Phys. F: Met. Phys.* **13** 1339
Flank A M, Raoux D, Naudon A and Sadoc J F *J. Non-Cryst. Solids* **61–62** 445
Goudeau P, Naudon A, Chamberod A, Rodmacq B and Williams C E 1987 *Europhys. Lett.* **3** 269
Guinier A and Fournet G 1955 *Small Angle Scattering of X-rays* (New York: Wiley)
Lamparter P and Steeb S 1988 *J. Non-Cryst. Solids* **106** 137
Lamparter P, Steeb S, Kroeger D M and Spooner S 1988 *Mater. Sci. Eng.* **97** 227
Lefèbvre S, Harmelin M, Quivy A, Bigot J, Calvayrac Y and Bellissent R 1988 *Z. Phys. Chem., NF* **157** 365
Lyon O and Simon J P 1986 *Acta Metall.* **34** 1197
—— 1987 *Phys. Rev.* B **35** 5164
Maret M, Chieux P and Hicter P 1988 *Z. Phys. Chem., NF* **157** 109
Maret M, Chieux P, Hicter P, Atzmon M and Johnson W L 1987a *J. Phys. F: Met. Phys.* **17** 315
Maret M, Pasturel A and Chieux P 1987b *J. Phys. F: Met. Phys.* **17** 2191
Rikvold P A and Gunton J D 1982 *Phys. Rev. Lett.* **49** 286
Sazaki S 1984 *National Laboratory for High-Energy Physics, Tsukuba, Japan., Report* KEK 83.22
Simon J P and Lyon O 1989 *Acta Metall.* at press
Simon J P, Lyon O and De Fontaine D 1985 *J. Appl. Crystallogr.* **18** 230
Stanley H E 1971 *Introduction to Phase Transitions and Critical Phenomena* (Oxford: Clarendon)
Tenhover M 1981 *J. Phys. F: Met. Phys.* **11** 2697
Yavari A R 1988 *Acta Metall.* **36** 1863